

## Failure behavior of Zircaloy-4 cladding after oxidation and water quench

Jun Hwan Kim <sup>\*</sup>, Myoung Ho Lee, Byoung Kwon Choi, Yong Hwan Jeong

*Advanced Core Materials Laboratory, Korea Atomic Energy Research Institute, P.O. Box 105, Yuseong, Daejeon 305-600, Republic of Korea*

Received 2 March 2006; accepted 25 October 2006

### Abstract

Simulated LOCA (loss of coolant accident) tests and subsequent mechanical tests on Zircaloy-4 cladding were carried out to evaluate the failure behavior of the cladding. Zircaloy-4 claddings were oxidized in a steam environment from 900 to 1250 °C for a given time period followed by a flooding of cool water to simulate LOCA tests. After the simulated LOCA test, the ductility of the oxidized cladding was evaluated by mechanical tests such as ring compression test and 3-point bend test. Evaluation of the absorbed contents such as hydrogen and oxygen were also carried out. The results showed that Zircaloy-4 cladding failed during thermal shock when the ECR (equivalent cladding reacted) value exceeded 20%. Lower boundary of brittle failure at thermal shock corresponds to 20% of ECR line calculated by the Baker–Just equation regardless of test temperature. On the other hand, boundary of ductile failure by the mechanical test did not followed after the ECR line. It rapidly decreased above 1000 °C to show that all Zircaloy-4 claddings behaved brittle fracture above 1150 °C when it oxidized at 300 s. Microstructural analysis revealed that boundary of ductile failure by the mechanical test fitted well when the absorbed oxygen content inside the prior- $\beta$  layer was below 0.5 wt%.

© 2006 Published by Elsevier B.V.

### 1. Introduction

Fuel cladding is a component which contains fuel pellets to prevent fission products from being released outside. Because of the advantage of a neutron economy, zirconium alloy is used for the fuel cladding. It is of importance that the fuel cladding should maintain its fuel integrity in a postulated design-based accident, as well as during a normal operation. In terms of this, a loss of coolant accident (abbreviated as LOCA) is treated as one of

the most important design-basis accidents in a light water reactor (LWR). When a LOCA occurs, the temperature of the fuel system rises so that the cladding undergoes an oxidation caused by the reaction of the mixture of water and steam. After a certain time interval, the emergency core cooling system activates, and water is injected to cool down the hot core, which is inevitably accompanied by a thermal shrinkage of the cladding. When the embrittled cladding cannot stand the stress involved, the cladding fragments, which results in a release of radioactive fission product. To maintain the fuel integrity under postulated LOCA conditions, the Nuclear Regulatory Commission (NRC) established the fuel safety criteria related to a LOCA, where the peak

<sup>\*</sup> Corresponding author.

*E-mail address:* [junkhim@kaeri.re.kr](mailto:junkhim@kaeri.re.kr) (J.H. Kim).

fuel temperature and the total oxidation cannot exceed 1204 °C and 17% level respectively [1]. However, such criteria have been founded by applying a safety margin based on the Hobson's ring compression test [2], and it is reported that there exist differences between the existing safety criteria and the behavior of a actual cladding [3,4].

The objectives in this study are to quantitatively analyze the failure behavior of the fuel cladding and to construct a failure map of the fuel cladding under a simulated LOCA situation. Cladding was oxidized at various temperatures and times followed by an injection of cool water. Mechanical tests, such as the ring compression test and the 3-point bend test were carried out at the oxidized cladding. Finally, mechanical test result after LOCA test was incorporated into the conventional failure map and the revised failure diagram of the fuel cladding was evaluated to quantitatively evaluate the failure behavior of the oxidized cladding.

## 2. Experimental

### 2.1. Simulated LOCA test

Fig. 1(a) shows an illustration of a facility used for simulated LOCA test. A 200 mm-long Zircaloy-4 tube, which respectively has 9.5 mm outer diameter and 0.57 mm of thickness, was used in this study. Composition of Zircaloy-4 was Zr–1.3Sn–0.2Fe–0.1Cr, whose microstructure was stress-relieved. A direct heating by the ohmic resistance was applied to heat the specimen up to 1265 °C. The length of the heated section of the specimen was 160 mm. Specimen temperature was measured by a pyrometer. Before the test, a temperature calibration of the pyrometer was performed by using an attached thermocouple on the specimen at the same time. The temperature profile of the pyrometer and the thermocouple calibration revealed that the differences were no more than about 3–5 °C during the entire test period. In addition, axial temperature profile along the specimen was measured. Temperature value at the point  $\pm 80$  mm from the midpoint revealed no more than  $\pm 20$  °C.

To simulate a LOCA condition, the specimen was oxidized in a flowing steam at a desired temperature and time. The steam injected before turning on the power. During the initial stage of heating, an overshoot of the temperature may occur that could affect the high temperature oxidation behavior of the specimen. To minimize the overshoot, a

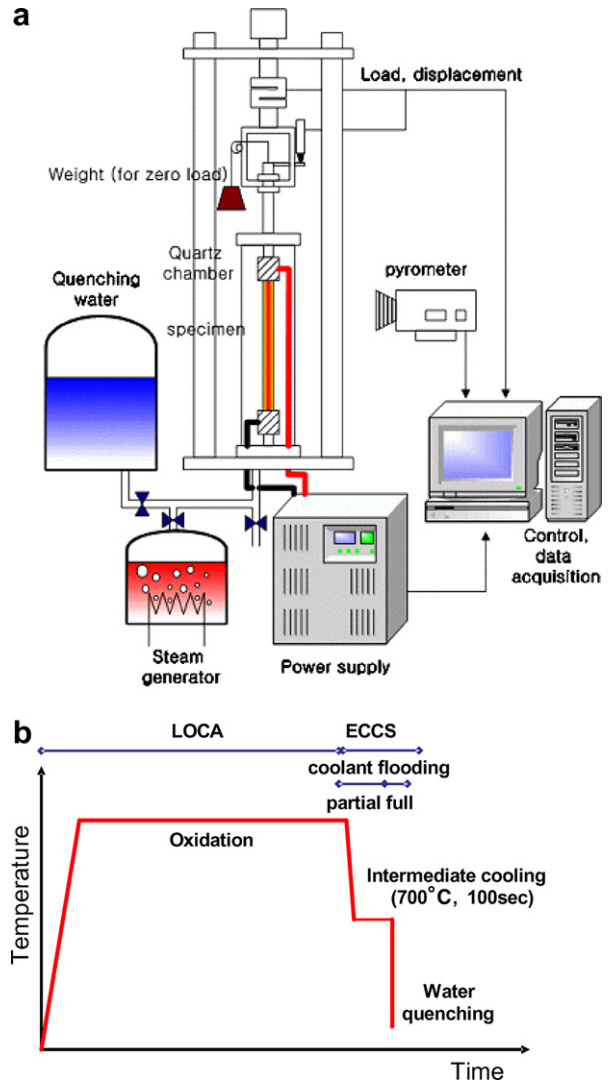


Fig. 1. Illustration of the LOCA simulation test: (a) test facility; (b) test scheme.

two-step heating was adopted. That is, a specimen was heated below the desired temperature in a short time to maintain the peak temperature below the test temperature, then it was heated to the desired temperature. When the cladding is exposed to an emergency coolant at the refill regime, a violent heat transfer between the hot cladding and cold water makes the coolant vaporize into steam, and the cladding temperatures do not abruptly drop until the sufficient coolant flooded the core. To simulate such a transient, the specimen was cooled at an intermediate temperature of 700 °C for 100 s after being oxidized, and then quenched. Such a transient is depicted in Fig. 1(b). During the test, the specimen may be subjected to unnecessary loads due to

an attached electrode, wire and connecting rod, etc. In order to compensate for such a load, a same weight was applied with a reverse direction to balance the net force in the test specimen to zero. All the data and procedures were collected and controlled by a computer.

In this study, two kinds of tests were introduced. First, the cladding was oxidized at the different temperatures but kept at the same time such as 300 s [5]. When the cladding is oxidized for the identical time but at the different temperature, the temperature where the material property abruptly decreases over the value is expected to be found, such as DBTT. Oxidized claddings were tested by using different kinds of mechanical tests to see which mechanical test was effective for assessing the embrittlement behavior (called ‘1-dimensional failure analysis’). Second, the claddings were oxidized at the different temperatures and times then the mechanical properties of the oxidized cladding was evaluated to construct a revised failure map of the zirconium cladding (called ‘2-dimensional failure analysis’). Detailed test schemes are shown in Table 1.

## 2.2. Mechanical tests

After the thermal shock test, ring compression test and 3-point bend test were performed to evaluate the oxidized cladding ductility. Ring compression test was selected because of its easiness. 3-point bend test was also selected because it is regarded to be more realistic than the ring compression. It is reported that it can simulate the axial buckling behavior of the cladding which is induced by an inadvertent operation during the handling of fuel bundles after the LOCA event [8]. Fig. 2 shows a schematic illustration of the mechanical tests. In the ring compression test, the oxidized cladding was cut into 15 mm length, and compressed by an Instron-type test machine at the rate of 1 mm per minute until a fracture. In the ring compression test, three specimens were collected at the middle part of

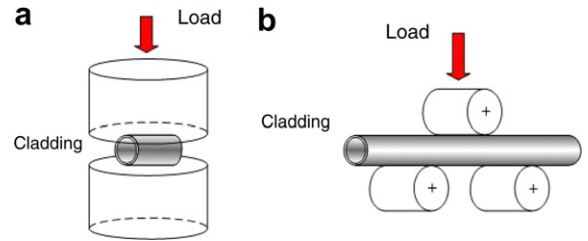


Fig. 2. Illustration of the mechanical tests: (a) ring compression test; (b) 3-point bend test.

the cladding then three identical tests were conducted. All data relating to the ring compression test were the average value of the three test results. In the case of the 3-point bend test, the oxidized cladding with a length of 180 mm was put into the bending jig then it was bent at the rate of 1 mm/min until a fracture. Span (distance between the loading jigs) length of the test was 70 mm. All the tests were performed at room temperature.

## 2.3. Microstructural analysis

When cladding is exposed to a high temperature steam environment, a diffusion of the oxygen results in the development of three distinct layers across the Zircaloy-4 cladding thickness, namely zirconium oxide, a stabilized alpha phase, and a prior- $\beta$  phase [3]. Fig. 3 shows the microstructure and local oxygen value of Zircaloy-4 cladding after oxidation and water quench. It can be shown that both oxygen content and local microhardness value decreased along the cladding thickness. Oxygen contents inside the prior- $\beta$  phase were constant throughout the thickness.

To determine the oxidation rate more quantitatively, the term ECR (equivalent cladding reacted) was introduced to be defined as the ratio of the converted metal thickness to the initial cladding thickness. Converted metal thickness can be defined as the equivalent metal thickness that would be

Table 1  
Experimental variables used in this study

	1-Dimensional failure evaluation	2-Dimensional failure evaluation
Oxidation temperature (°C)	900, 950, 1000, 1050, 1100, 1150, 1200, 1250, 1265 °C	900, 950, 1000, 1050, 1100, 1125, 1150, 1175, 1200, 1225, 1250 °C
Oxidation time (s)	Same at 300 s	300, 500, 1000, 2000, 3000, 5000, 7000, 10000, 15000 s
Mechanical test	Ring compression test 3-point bend test	3-Point bend test
Microstructural analysis	Hydrogen analysis oxygen analysis	Hydrogen analysis oxygen analysis

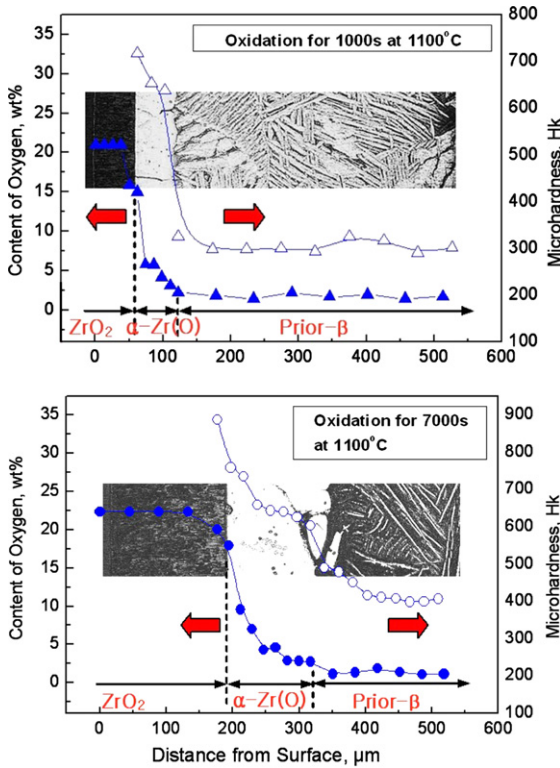


Fig. 3. Local microhardness, oxygen content, and the microstructure of Zircaloy-4 cladding after oxidation and water quench.

converted to oxide if all the oxygen absorbed by and reacted with the cladding is locally converted to stoichiometric zirconium [1]. Using a dimensional conversion, the ECR value of zirconium can be derived according to the relationship

$$\begin{aligned}
 \text{ECR}(\%) &= \frac{t_m}{t_i} \times 100 = \frac{\Delta m_{\text{Zr}}}{\rho_{\text{Zr}} \cdot t_i} \times 100 \\
 &= 2.693 \times 10^{-3} \Delta m_{\text{Zr}} \\
 &= 2.693 \times 10^{-3} \cdot (3.36 \times 10^{11} \\
 &\quad \times \exp(-22900/T) \times t)^{0.5}, \quad (1)
 \end{aligned}$$

where  $t_i$ : initial thickness of zirconium cladding;  $t_m$ : thickness of zirconium reacted during oxidation;  $\Delta m_{\text{Zr}}$ : total mass change of zirconium metal (in mg/dm<sup>2</sup>);  $\rho_{\text{Zr}}$ : density of the zirconium;  $T$ : oxidation temperature (in K);  $t$ : oxidation time (in s).

To calculate the ECR value, the Baker–Just equation [6], which is used as a reference oxidation model of zirconium by NRC, was adopted as the weight gain formula in this study. Hydrogen and oxygen pickup occur at the cladding surface as the

oxidation proceeds, and they diffuse and penetrate into the cladding to play an important role in the mechanical properties. Absorbed hydrogen content in the oxidized cladding was measured by a gas analysis method. Three or four specimens were sampled at the middle part of the cladding. Prior to the hydrogen analysis, they were ultrasonically treated in the acetone to remove surface grease then they were treated in the carbon tetrachloride solution to remove the surface moisture that greatly affects hydrogen content. Regarding the absorbed oxygen, the thickness of the prior-β phase and its associated oxygen content have a great influence on the cladding integrity against a thermal shock [3]. Since the local oxygen value measured by an EDX shows only the relative value, it was decided to measure the ‘absolute’ oxygen value at the prior-β phase by removing surface oxide then analyzing it by gas analysis. Several specimens after thermal shock test were sampled and cut into small parts. They were ground on both sides to remove the surface oxide, leaving up to a thickness of 50 μm, and an attempt to measure the oxygen content inside the prior-β layer was initiated. As shown in Fig. 3, thickness of prior-β phase was in the range of 200–400 μm so that ‘the pure prior-β layer’ is expected to obtain once it has carefully ground much at outer surface but little at inner surface to thin it down to 50 μm. Similar to the hydrogen analysis, several oxygen contents from the single specimen were analyzed and averaged.

### 3. Results and discussion

#### 3.1. Mechanical test

Fig. 4 shows the load–displacement curves of the oxidized cladding from the ring compression test and the 3-point bend test. In the ring compression result, the cladding oxidized at 900 °C exhibited a ductile compression during the test. In the cladding oxidized over 950 °C, however, the cladding showed an abrupt load drop then it showed a plastic deformation at the rest of the curve. Such a load drop is mainly due to a fracture of the brittle oxide outside the cladding surface. Thickness of the oxide below 900 °C was so thin that it cannot affect the deformation behavior of the cladding. However, when oxidized above 950 °C, the oxide growth and its thickness became so significant that the load drop cannot be neglected. Even when a load drop occurred, the prior-β layer was so stable that it

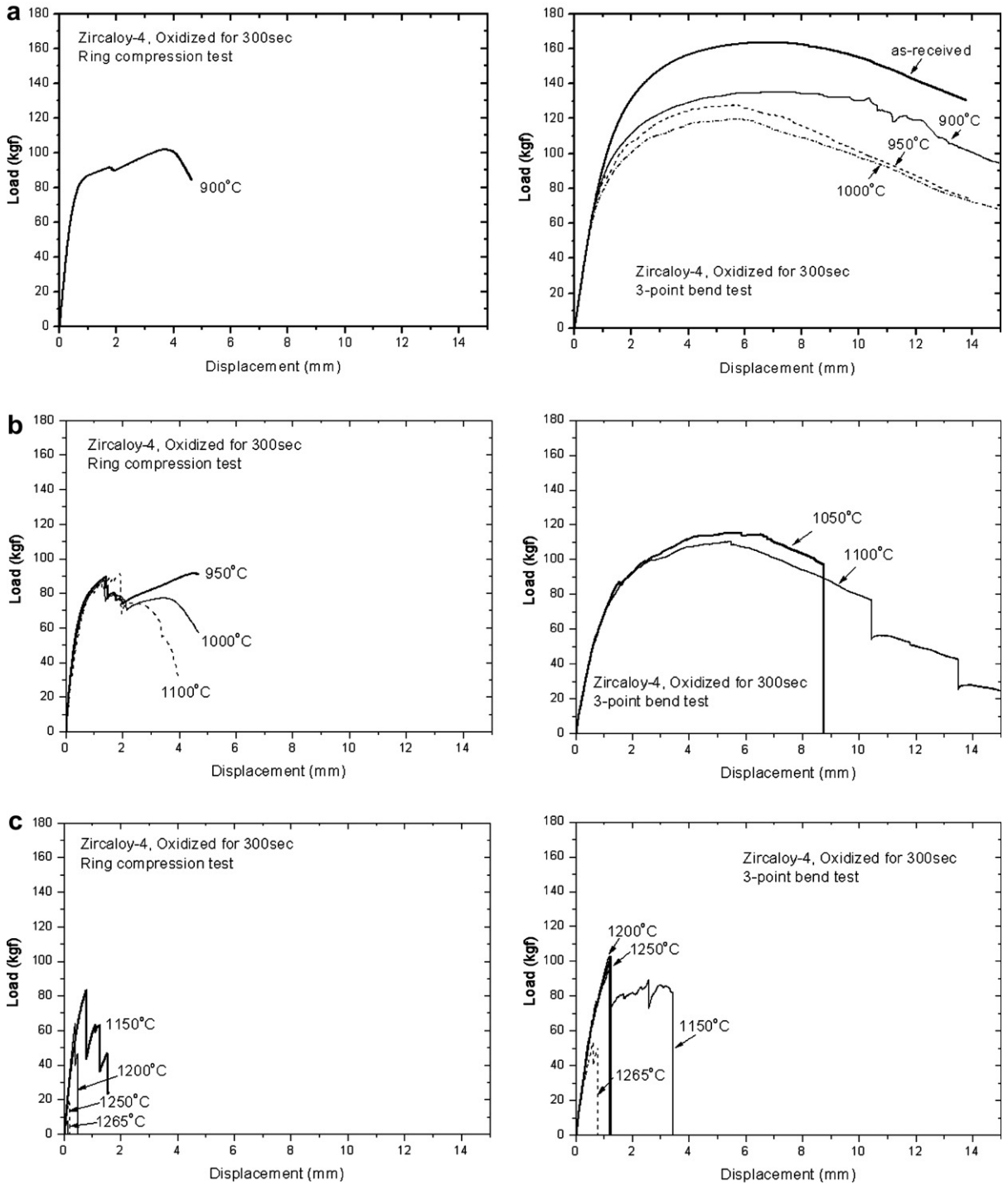


Fig. 4. Load–displacement curve of the Zircaloy-4 cladding after the thermal shock test using both ring compression and 3-point bend test: (a) ductile deformation; (b) load drop at plastic region; (c) load drop at elastic region.

can sustain an additional compression load. Additional load after load drop gradually decreased as the oxidation temperature increases to 1100 °C. In

the oxidized cladding beyond 1150 °C, the thickness of prior-β layer was so thin as well as brittle that it showed a load drop at the elastic region. However,



load increases again after the first load drop to result in a sawtooth-type pattern. The reason why the successive load increase and drop occur is that ring compression specimen can resist further compression because the specimen, although it fractured, still maintains cylindrical shape rather than breaks in pieces. When oxidized over 1200 °C, the cladding was severely embrittled such that it could not maintain the first load drop and it showed a brittle failure.

In the case of the 3-point bend test as shown in Fig. 4, the overall trends do not much differ from that of the ring compression test. In the cladding oxidized below 1000 °C, the cladding shows a simple bending without showing any load drop or brittle failure. Cladding oxidized at 1000 °C showed a smaller load when compared to the 900 °C specimen, which is due to a reduction of the load bearing area inside the zirconium cladding. When oxidized between 1050 °C and 1100 °C, it failed after it reaches above maximum load. Above 1150 °C, the cladding exhibited a brittle failure without showing any sawtooth pattern as in the ring compression test. It failed at a small flexural displacement before reaching the maximum load.

Fig. 5 shows the changes of the mechanical properties such as the maximum load and displacement with the oxidation temperature. Ductile compression or bending is shown when the cladding is oxidized at a relatively low temperature ('ductile deformation' region). Load drops caused by a fracture of the surface oxide occurred at the plastic region when the cladding was oxidized at the intermediate temperature region ('load drop at plastic region' region). Finally, a load drop occurred at the elastic region to show that brittle fracture which could not sustain the first load drop appeared when the cladding was oxidized at a high temperature ('brittle failure at elastic region' region). Maximum load in the ring compression decreased slowly as the temperature increased then it decreased rapidly above the brittle failure region. On the other hand, the maximum load in the 3-point bend specimen decreases slowly until 1200 °C.

Besides the maximum load, the maximum displacement also decreased with the oxidation temperature. Maximum displacement was taken at the point where the first load drop occurred from the load–displacement curve. Maximum displacement cannot be measured at the specimen like 900 °C in ring compression and below 1000 °C in 3-point bend test, because no load drop is found at the clad-

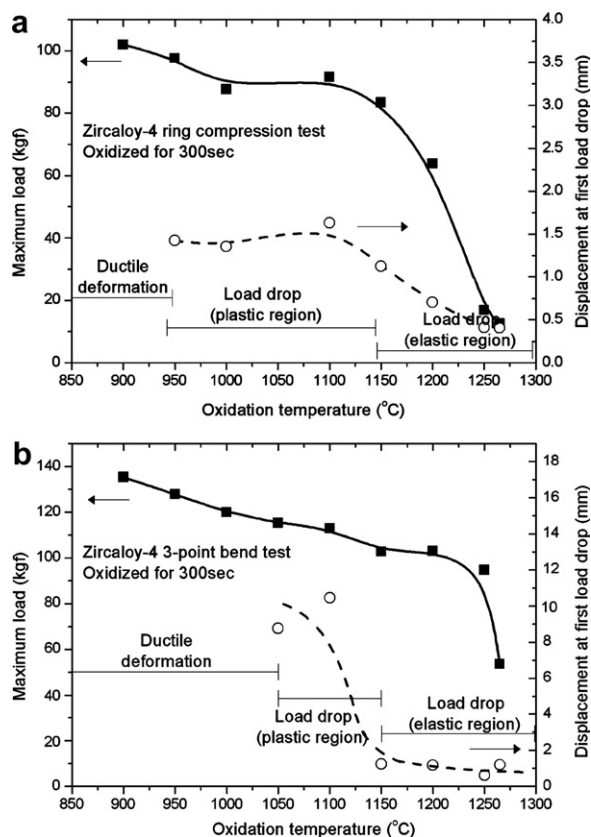


Fig. 5. Changes of the mechanical properties of the fuel cladding with the oxidation temperature: (a) ring compression test; (b) 3-point bend test.

ding which shows ductile deformation. Maximum displacement in the ring compression specimen continuously decreased with the oxidation temperature, whereas the 3-point bend specimen showed an abrupt decrease of the displacement above the 'brittle failure region'. In the ring compression test, ring geometry is maintained throughout the test to exhibit sawtooth pattern in load–displacement curve. In the case of 3-point bend test, however, cladding will break in pieces above the fracture load, which leads to the abrupt displacement decrease over the 'load drop' region.

### 3.2. 1-Dimensional failure analysis

Fig. 6 shows the behavior of the absorbed energy during the mechanical test with the oxidation temperature, where oxidation time was set constant for 300 s. Absorbed energy can be defined as the area under the load–displacement curve which has a dimension of the energy. Both energies obtained

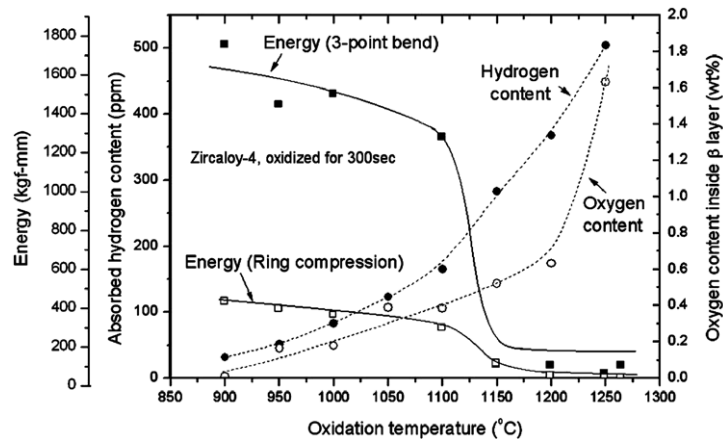


Fig. 6. Changes of the absorbed energy and the absorbed contents of the fuel cladding with the oxidation temperature.

by the ring compression and 3-point bend tests decreased with the oxidation temperature, and they showed an abrupt decrease between 1100 and 1150 °C. Energy of the 3-point bend specimen was larger than that of the ring compression because the specimen size of the bend test is larger than that of the compression test. From this result, one can conclude that the 3-point bend test is more sensitive for evaluating the failure criterion in that the changes of the absorbed energy are more distinct than in the ring compression test.

Fig. 6 also shows the changes of the absorbed contents of the Zircaloy-4 cladding with the oxidation temperature. Both the absorbed hydrogen content and the oxygen content inside the prior-β layer increased with the oxidation temperature. Absorbed hydrogen content gradually increased in all the temperature regions. Hydrogen content, when the Zircaloy-4 cladding oxidized at the 1150 °C above which it exhibited a brittle fracture, shows 270 ppm. Oxygen content inside the prior-β layer increased slowly below 1200 °C then it increased rapidly above this temperature. Oxygen content at 1150 °C, above which it showed brittle fracture, was 0.5 wt%. It can be said that the oxygen content of the cladding to show a brittle fracture is above 0.5 wt%. Thus the cladding cannot withstand the load to show nil ductility when the absorbed oxygen content inside the β layer exceeds 0.5 wt%. When compared to the oxygen content inside the prior-β phase from the pseudo-binary phase diagram of Zircaloy-4 and oxygen [7], the absorbed oxygen content in this study was similar to the theoretical oxygen solubility below 1200 °C. At 1250 °C, the actual oxygen value increased so high as to reach

around 1.6 wt%, whereas the maximum oxygen solubility corresponding to this temperature is 0.7 wt%. It seemed that the temperature was so high as to result in the accelerated oxygen diffusion occurred above 1200 °C to exceed in the oxygen content inside the prior-β phase in which the cladding leads to a brittle failure.

### 3.3. 2-Dimensional failure analysis

Fig. 7 shows the failure behavior of Zircaloy-4 cladding after the thermal shock test with various oxidation temperatures and times. Open and closed symbols respectively denote the specimens which survived and failed after a cold water injection followed by a high temperature oxidation. When the heated cladding was quenched by the cold water, the cladding undergoes thermal shrinkage so that the length of the cladding abruptly reduced. Slightly oxidized cladding which has either low temperature or short oxidation time can accommodate such shrinkage to maintain its integrity during the quench. However, heavily oxidized cladding like either high temperature or long oxidation time cannot maintain the shrinkage then it fails during the water quench. Oxidized cladding during quenching usually fails by cutting in halves across the cladding diameter. In the case of heavily oxidized claddings, they are shattered in pieces immediately after cold water injection. Solid curve represents the ECR value calculated from the Baker–Just equation. Zircaloy-4 cladding oxidized at 1000 °C does not fail until the oxidation time exceeds 10000 s. As the oxidation temperature increases, oxidation time to cause a failure decreases such as

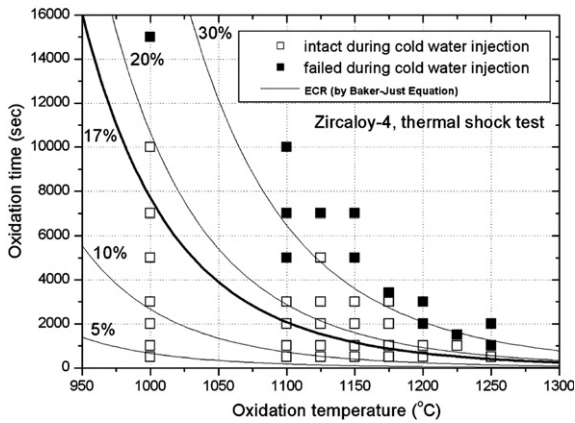


Fig. 7. Failure map of the Zircaloy-4 cladding after the thermal shock test.

1100 °C in 5000 s and 1200 °C in 2000 s. The minimum ECR which is defined as the minimum point where a cladding fails, lies between 20% and 30%, indicates that the conventional 17% ECR criteria for a cladding failure is somewhat conservative.

Fig. 8 is the 2-dimensional failure diagram of the Zircaloy-4 cladding according to the Arrhenius form when collated with the calculated 3-point bend energy based on the previous section. Same in the Fig. 7, closed symbol represents the failed cladding during the water quench. The ductile bending can be easily distinguished from the brittle fracture in that absorbed energy in the ductile bending lies in the value over 1200 kgf-mm, whereas 100 kgf-mm ranges in the brittle failure region. When separating each region based on the fracture energy, one can

obtain the empirical failure behavior of the Zircaloy-4 cladding under the LOCA condition. ‘Ductile bending’ (blue<sup>1</sup> region in Fig. 8) means that the cladding can assure its mechanical ductility after a thermal shock, not to mention a survival during a water quenching. ‘brittle fracture at the mechanical test’ (green region in Fig. 8) means that although the cladding at first survived the water quenching, it has already lost its mechanical ductility so that it could be failed during a handling, such as refueling or transporting the fuel bundles to the spent fuel storage [8]. ‘Brittle failure at a thermal shock’ (red region in Fig. 8) indicates that the cladding is too brittle to withstand even a thermal stress during a water quenching. From the diagram, ‘ductile bending’ region decreases with the oxidation temperature. For instance, a ductile bending occurs irrespective of the oxidation time when oxidized below 950 °C. However, it loses its mechanical ductility above 5000 s when oxidized at 1000 °C. Finally, oxidized cladding at 1150 °C shows its mechanical ductility only at 300 s. The maximum ECR to withstand a ductile bending is around 15% when oxidized at 1000 °C. It gradually decreases to have a ECR below 10% when oxidized above 1100 °C.

Fig. 9 shows the changes of the absorbed content when collated with the Arrhenius form of the failure map. When connecting each of the same values, such as drawing the contours, an empirical diagram of each absorbed contents can be obtained. In this diagram, the effect of the hydrogen on the failure behavior of the Zircaloy-4 cladding was low. Instead, the trends of the absorbed oxygen inside the prior-β layer fit well with the cladding ductility region (refer to the blue region in Fig. 8). Cladding whose oxygen contents in the prior-β layer are less than 0.5 wt% showed a ductile failure, which exactly corresponds to the result of the 1-dimensional failure analysis as mentioned in the previous section.

So far, the approach on the construction of the revised failure diagram, where the thermal shock test was combined with the mechanical test, can be extended to the other studies. That is, revised failure diagram as proposed in this study can be extended to the condition where cladding ballooned prior to high temperature oxidation, axially constrained condition, high-burnup condition such as pre-hyd-

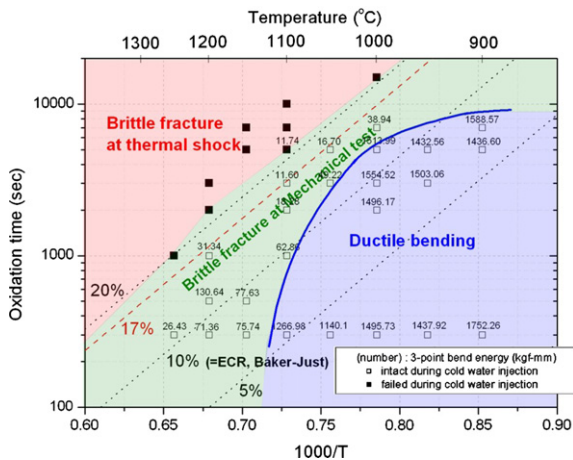


Fig. 8. Changes of the 3-point bend fracture energy of the fuel cladding with the oxidation temperature and time.

<sup>1</sup> For interpretation of color in Fig. 8, the reader is referred to the web version of this article.



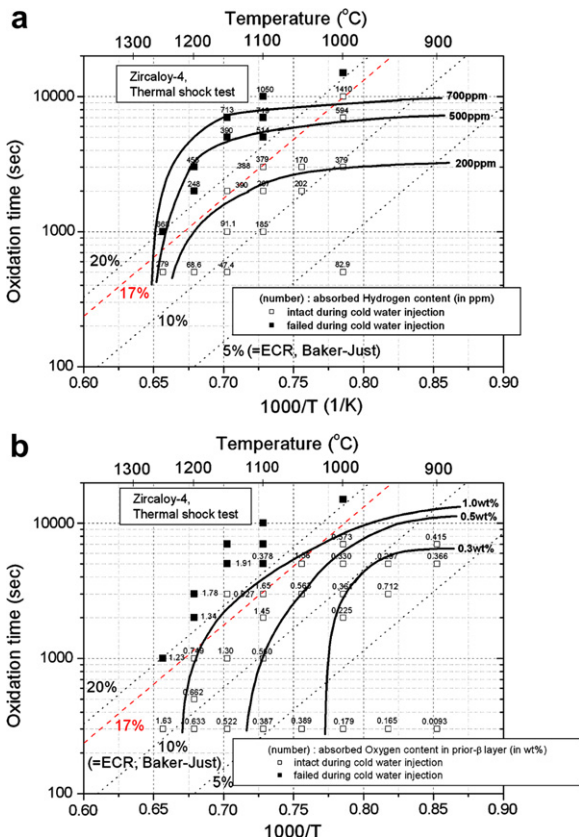


Fig. 9. Changes of the material properties of the fuel cladding with the oxidation temperature and time: (a) absorbed hydrogen content (b) oxygen content inside prior- $\beta$  layer.

ridged cladding, and Nb-contained advanced cladding. Quantitative evaluation how each region (ductile bending, brittle fracture at the mechanical test, and brittle fracture at thermal shock) will be changed with the change of condition (ballooning, axial stress, pre-hydride, and Nb content, and so on) will be of importance. For example, the existence of hydride inside zirconium matrix generated during normal operation will induce small decrease in the minimum ECR above which cladding will fail during thermal shock (red region would be little changed compared to the as-received condition). However, it is expected that large decrease in the threshold ECR above which oxidized cladding will show brittle failure at the mechanical test (blue region would shrink rapidly compared to the as-received condition), because pre-hydride increases oxygen content inside the prior- $\beta$  layer to rapidly decrease mechanical ductility of the oxidized and quenched cladding [9].

#### 4. Conclusion

To analyze the failure behavior of Zircaloy-4 cladding under a LOCA condition, a simulated LOCA test and subsequent mechanical tests were conducted. After conducting the thermal shock test at the temperature ranges from 900 to 1250 °C with various times followed by mechanical tests and a microstructure analysis, the following were obtained:

- (1) 3-Point bend test is more sensitive than the ring compression test in assessing the failure behavior of an oxidized cladding.
- (2) The minimum ECR of the Zircaloy-4 cladding to cause a brittle fracture during thermal shock is around 20%, regardless of oxidation temperature. On the other hand, threshold ECR, below which mechanical ductility of the cladding can be assured, decreased as the oxidation temperature increased.
- (3) The absorbed oxygen contents in the prior- $\beta$  layer had an influence on the 3-point absorbed energy. When the absorbed oxygen content was less than 0.5%, the cladding maintained its mechanical ductility after the LOCA test.

#### Acknowledgement

This study was supported by Korea Science and Engineering Foundation (KOSEF) and Ministry of Science and Technology (MOST), Korean Government, through its national nuclear technology program.

#### References

- [1] Nuclear Regulatory Commission, 10 CFR 50.46, Acceptance Criteria for Emergency Core Cooling Systems for Light Water Nuclear Power Reactors, 1973.
- [2] D.O. Hobson, P.L. Rittenhouse, Embrittlement of Zircaloy Clad Fuel Rods by Steam during LOCA Transients ORNL-4758, 1972.
- [3] H.M. Chung, T.F. Kassner, Embrittlement Criteria for Zircaloy Fuel Cladding Applicable to Accident Situations in Light-Water Reactors: Summary Report NUREG/CR-0344, 1980.
- [4] F. Nagase, T. Fuketa, recent results from LOCA study in JAERI, in: Proceedings of the 2003 Nuclear Safety Research Conference NUREG/CP-0185, 2003.
- [5] C. Vitanza, Consideration on LOCA Criteria including High Burn-up Effect, SEGFSM Topical Meeting on LOCA Issues, Argonne National Laboratory, May 25–26, 2004.

- [6] L. Baker, L.C. Just, Studies of Metal–Water Reactions at High Temperatures III. Experimental and Theoretical Studies of the Zirconium–Water Reactions, ANL-6548, 1962.
- [7] H.M. Chung, T.F. Kassner, *J. Nucl. Mater.* 84 (1979) 327.
- [8] A. Machiels, Perspective on Requirements for Spent Fuel Storage and Transportation, Nuclear Safety Research Conference 2004, 2004.
- [9] J.H. Kim, B.K. Choi, J.H. Baek, Y.H. Jeong, *Nucl. Eng. Des.* 236 (2006) 2386.